Oceanic and atmospheric transport of multiyear El Niño–Southern Oscillation (ENSO) signatures to the polar regions

S. Jevrejeva,[1] J. C. Moore,[2] and A. Grinsted[2,3]

[1] Using Monte-Carlo Singular Spectrum Analysis (MC- SSA) and Wavelet Transform (WT) we separate statistically significant components from time series and demonstrate significant co-variance and consistent phase differences between ice conditions and the Arctic Oscillation and Southern Oscillation indices (AO and SOI) at 2.2, 3.5, 5.7 and 13.9 year periods. The 2.2, 3.5 and 5.7 year signals detected in the Arctic are generated about three months earlier in the tropical Pacific Ocean. In contrast, we show that the 13.9 year signal propagates eastward from the western Pacific as equatorial coupled waves (ECW, $0.13-0.15 \text{ ms}^{-1}$), and then as fast boundary waves $(1-3 \text{ ms}^{-1})$ along the western margins of the Americas, with a phase difference of about $1.8-2.1$ years by the time they reach the Arctic. Our results provide evidence of dynamical connections between high latitude surface conditions, tropical ocean sea surface temperatures mediated by tropical wave propagation, the wintertime polar vortex and the AO. *INDEX TERMS:* 1620 Global Change: Climate dynamics (3309); 3309 Meteorology and Atmospheric Dynamics: Climatology (1620); 0312 Atmospheric Composition and Structure: Air/sea constituent fluxes (3339, 4504); 4504 Oceanography: Physical: Air/sea interactions (0312); 4522 Oceanography: Physical: El Nino. **Citation:** Jevrejeva, S., J. C. Moore, and A. Grinsted (2004), Oceanic and atmospheric transport of multiyear El Niño–Southern Oscillation (ENSO) signatures to the polar regions, *Geophys. Res. Lett.*, *31*, L24210, doi:10.1029/2004GL020871.

1. Introduction

[2] Several studies indicate that the relationships between the El Niño-Southern Oscillation (ENSO) and climate anomalies in the North Atlantic (NA) sector are both weak and ubiquitous, however most evidence of linkage comes from model simulations [e.g., *Trenberth et al.*, 1998; *Merkel and Latif*, 2002] or from 50 years of reanalysis data [*Ribera and Mann*, 2002]. What is missing is clear observational evidence, especially spanning long time periods. Impacts of ENSO are more plausibly seen in the NA sector during winter than summer, though the signal to noise ratio is rather low [*Trenberth et al.*, 1998; *Huang et al.*, 1998; *Pozo-Vázquez et al.*, 2001]. These considerations motivated us to use the NH time series of ice conditions and advanced statistical methods to extract signals associated with ENSO. Our idea is that ENSO signals can be extracted from the ice conditions time series, since ice extent is an integrated parameter of winter seasons and acts as a non- linear filter for $2-13$ year oscillations during the winter seasons [*Jevrejeva and Moore*, 2001]. ENSO quasi-biennial (QB) and quasi- quadrennial (QQ) signals were detected by Monte Carlo Singular Spectrum Analysis (MC-SSA) in time series of the Northern Hemisphere (NH) annular mode (NAM) and ice conditions in the Baltic Sea [*Jevrejeva and Moore*, 2001], which are consistent with results obtained for the time series of sea ice cover from the Arctic and Antarctic [*Gloersen*, 1995; *Venegas and Mysak*, 2000]. This paper focuses on the dynamic linkages, and putative mechanisms, especially for the low frequency component (13.9 year signal), between the ENSO and NAM circulation indices and between the NH ice conditions and polar/tropical circulation patterns over the past 150 years using the MC-SSA and crosswavelet and wavelet coherence methods.

2. Data

[3] We used a 135-year time series of the monthly SOI [*Ropelewski and Jones*, 1987], as the atmospheric component of ENSO and the Niño3 SST index (1857–2001) [*Kaplan et al.*, 1998], defined as the monthly SST averaged over the eastern half of the tropical Pacific (5°S–5°N, 90°–150°W) as the oceanic part. To ensure the robustness of the results, we repeated the analyses for the monthly Niño1+2 (0°–10°S, 90°–80°W) and monthly Niño3.4 (5°S–5°N, 170°–120°W) time series [*Kaplan et al.*, 1998]. NAM was represented by the monthly AO index based on the pressure pattern (1899–2001) [*Thompson and Wallace*, 1998] and the extended AO index (1857–1997) based on the pattern of surface air temperature anomalies [*Thompson and Wallace*, 1998].

[4] Measures of winter season severity come from the time series of maximum annual ice extent in the Baltic Sea (BMI), 1857–2000 [*Seinä and Palosuo*, 1996], April ice extent in the Barents Sea (BE: Eastern part 10°–70°E; and BW: Western part 30°W–10°E), 1864–1998 [*Venje*, 2001] and the date of ice break-up at Riga since 1857 [*Jevrejeva and Moore*, 2001]. Global SST since 1854 were taken from the Extended Reconstructed Sea Surface Temperature (ERSST) [*Smith and Reynolds*, 2003] 2° × 2° dataset down-sampled to yearly values.

3. Methods

[5] The analysis is performed using MC-SSA [*Allen and Smith*, 1996] and wavelet transform (WT) with a Morlet wavelet [*Foufoula-Georgiou and Kumar*, 1995]. We applied MC-SSA to calculate the contribution from non-linear long-term trends and quasi-regular oscillations to total variance, and analyse their development over time. We used the WT to determine both the dominant modes of variability and

[1]Proudman Oceanographic Laboratory, Birkenhead, UK.
[2]Arctic Centre, University of Lapland, Rovaniemi, Finland.
[3]Also at Department of Geophysics, University of Oulu, Oulu, Finland.

Table 1. Contribution From Significant Components Detected by MC-SSA in Time Series of SOI, Niño3, AO, and Ice Conditions to the Total Variance[a]

Contribution (%)	Period (years)			
	2.2	3.5	5.7	13.9
SOI	3	27	18	4
Niño3		**3**	**7**	4*
AO	**9**		3	6
Barents sea		1	2	4
Baltic sea	5	**3**	4	3
Riga	**4**	4	5	**5**

[a]Rows in bold indicate EOFs at 95% in an AR(1) red-noise model, * indicate EOFs at 90% level, others are significant at 95% level in white noise models.

how those modes vary in time. Statistical significance was estimated against a red noise model. We calculated a coherence measure of the intensity of the covariance of the two series in time-frequency space [*Torrence and Webster*, 1999]. Phase difference between the components of the two time series was estimated as the circular mean of the phase for those regions with higher than 5% statistical significance and which are outside the cone of influence [*Jevrejeva et al.*, 2003].

4. Results

[6] Decomposition of time series of SOI, Niño3, AO and ice conditions are presented in Table 1. Signals with 2.2, 3.5, 5.7 and 13.9 year periodicities were detected in ice conditions time series and associated with similar signals in SOI/Niño3. Results are consistent with QB and QQ detected by [*Gloersen*, 1995; *Venegas and Mysak*, 2000] in shorter time series of ice conditions in polar regions and with signals in SST and sea level pressure (SLP) anomalies over the Pacific Ocean [*Huang et al.*, 1998; *Torrence and Webster*, 1999; *White and Tourre*, 2003; *Ribera and Mann*, 2002]. As expected, the signals, detected in ice time series, are rather weak; with 1–6% contribution to the total variance, however, this amounts to 20–25% of all statistically significant signals (Table 1).

[7] To investigate the direct link between the localised signals from atmospheric circulation index and ice conditions we use crosswavelet and coherency methods. Results for the Barents Sea ice conditions with AO/Niño3 (Figures 1a
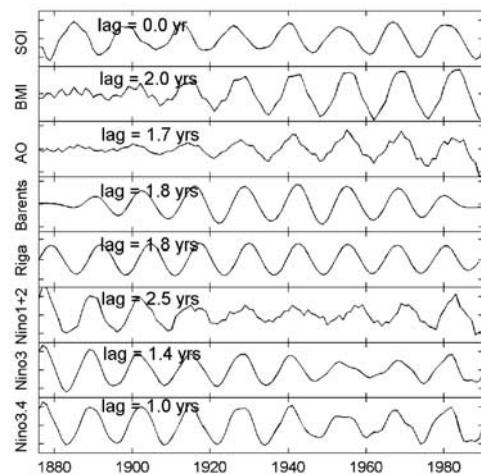

Figure 2. 13.9 year signals from time series of SOI, ice extent in the Baltic Sea, AO, ice extent in the Barents Sea, time series of date of ice break-up at Riga, Niño1+2, Niño3, Niño3.4.

and 1c) and Baltic Sea with AO/SOI (Figures 1b and 1d) show that the phase lag where coherency >0.8 (corresponding to the 95% significance level) is consistently about 3 months for the 2.2–5.7 year signals. The same lag has also been found for the NA region [*Pozo-Vázquez et al.*, 2001].

[8] Wavelet coherence between SOI, Niño3, AO and ice conditions is significant in the 12–20 year band. Using MC-SSA we isolated the 13.9 year oscillations in time series (Figure 2). The phase relationship between the oscillations was then determined by cross spectral density estimates (relative to SOI). The 13.9 year SOI signal leads the AO by 1.7 years and ice conditions by 1.8–2.1 years. We also found a 1.4 year lag between the 13.9 year signals from SOI and Niño3. The different phase relationship between signals with periodicities of 2.2–5.7 and 13.9 years suggests different mechanisms of signal propagation from the equatorial Pacific Ocean to the polar regions for the 13.9 year signal and for the shorter period ones.

[9] The mechanism linking between the QB oscillations (2.2–3.5 years) signals detected in ice conditions time series and in tropical forcing, has been described by *Baldwin and Dunkerton* [2001], as extra-tropical wave propagation,
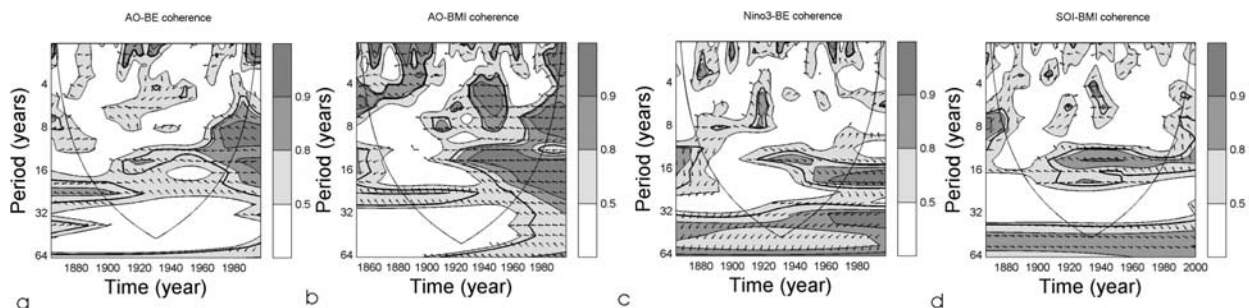

Figure 1. The wavelet coherency and phase difference between AO/ice extent in the Barents Sea (a). Contours are wavelet squared coherencies. The vectors indicate the phase difference a) horizontal arrow pointing from left to right signifies in-phase and an arrow pointing vertically upward means the second series lags the first by 90 degrees (i.e., the phase angle is 270°); b) the same for the AO/ice extent in the Baltic Sea; c) the same for the Niño3/ice extent in the Barents Sea; d) the same for the SOI/ice extent in the Baltic Sea.

affecting breakdown of the wintertime stratospheric polar vortices. Since the AO may be interpreted as a physical phenomenon associated with the structure of the polar vortex and related changes in the stratospheric and tropospheric pressure fields and the stratospheric polar vortex affects surface weather patterns, the QBO has an effect on high latitude weather patterns [*Baldwin and Dunkerton*, 2001; *Castanheira and Graf*, 2003]. The marked similarity in the phase lag of the 5.7 year signal to that of QB signal in SOI and ice conditions strongly suggests a similar mechanism of propagation.

[10] We hypothesize that the lag between SOI and Niño3 signals can be explained by propagation of ECW on a decadal scale [*White et al.*, 2003; *Capotondi and Alexander*, 2001], from off-equatorial wind stress curl and triggered ECW by reflected coupled Rossby waves (CRW). We consider Rossby waves as a solution to the problem of adjustment of the geophysical fluid to large-scale perturbation, based on the conservation of angular momentum. *Wang and Weisberg* [1994] found that ECW propagate eastward across the Pacific at speed of 0.28 ms^{-1}. *White et al.* [2003] showed the existence of coupled waves occurring in response to Rossby wave reflection on the western boundary that propagate eastward with phase speeds of about 0.12 ms^{-1} on decadal period scales. These waves propagate slowly eastward along the equator in the Pacific Ocean in concert with global SST/SLP waves. To investigate these decadal-scale waves, on the assumption that they are identifiable in the 13.9 year signals found in the SOI and Niño3 series, we analysed the phase difference between the 13.9 years signals from SOI, Niño3, Niño1+2 and Niño3.4 calculated by MC-SSA (Figure 2). The results provide evidence of an increase of phase difference for 13.9 year signals with eastward propagation. Using these lags gives an eastward propagation speed of 0.13–0.17 ms^{-1} for 13.9 year signals along the equator, which is in excellent agreement with the speed of decadal-period ECW described by *White et al.* [2003].

[11] We have projected the 13.9 year signal extracted from SOI on the SST anomalies in the Pacific (1854–1997) (Figure 3). The strength of correlation and the phase of correlation maps illustrate a meridional V-shape pattern, which is symmetric along the equator, propagating eastward across the ocean, with a speed of 0.15 ms^{-1} interrupted in the central tropical Pacific Ocean by the development of anomalous warm/cool tongues. When ECW reach the margins of North and South America they transform to baroclinic Kelvin boundary waves (KBW), propagating polewards [*Enfield and Allen*, 1980; *Meyers et al.*, 1998], of which the most energetic waves can reach as far north as Alaska [*Meyers et al.*, 1998]. They are thought to start near the equator with Kelvin wave-like structure, and evolve towards a continental shelf wave structure at higher latitudes [*Suginohara*, 1981]. This mechanism is well-established for equatorial Kelvin waves. For ECW, the excitation of boundary Kelvin waves may be due to a combination of the incoming ocean signal and forcing by coupled wind stress at the boundary (*Clark* [1992] suggested that wind stress becomes relatively more important at longer periods).

[12] Fast poleward propagation of KBW (a few months) is confirmed by the phase angle map (Figure 3b), where we can trace the propagation along the western margin of South
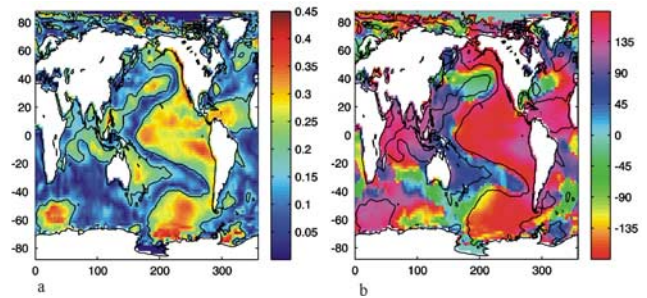

Figure 3. Map of magnitude of correlation between SST and the in-phase and quadrature 13.9 year SOI cycle, 95% significance is delineated by the black line (a). Map of relative phase angle (degrees) between the SST and in-phase and quadrature SOI 13.9 year cycle (b).

and North America and also along the Arctic continental shelf.

[13] A noticeable feature of Figure 3 is the strong 13.9 year signal around the Antarctic, a similar 13.9 year signal was reported as a long-standing feature in 2000 year ice core record from the Antarctic [*Fischer et al.*, 2004], which they ascribed to a mode of variability in the Antarctic Circumpolar Wave (ACW). However, the ACW has also been thought of as an ENSO teleconnnection, and *Park et al.* [2004] argue strongly that it is a geographically phase-locked standing wave train linked to tropical ENSO episodes. This ENSO-modulated quasi-stationary variability is not zonally uniform, rather, the strongest ENSO impact is consistently concentrated in the Pacific sector of the Southern Ocean, as we observe in Figure 3.

5. Conclusion

[14] We provide evidence of ENSO influence on the winter climate variability in NH during the last 150 years via signals in the 2.2, 3.5, 5.7 and 13.9 year bands. The contribution from the signals to the total variance is relatively weak, varies considerably with time, but is statistically significant. Phase relationships for the different frequency signals suggest that there are different mechanisms for distribution of the 2.2–5.7 year and the 13.9 year signals. The 2.2–5.7 year signals are most likely transmitted via the stratosphere, and the AO mediating propagation of the signals, through coupled stratospheric and tropospheric circulation variability that accounts for vertical planetary wave propagation.

[15] The delay of about two years in the 13.9 year signals detected in polar region can be explained by the transit time of the 13.9 year signal associated with ECW (0.13–0.17 ms^{-1}) propagation in the Pacific ocean, KBW (1–3 ms^{-1}) propagation along the western margins of the Americas and by poleward-propagating of atmospheric angular momentum [*Dickey et al.*, 2003]. This mechanism is supported by similar features in the Pacific sector of the Antarctic SST field.

[16] Our results highlight the importance of tropical variations for the Arctic and NA climate and probably at least the Pacific sector of the Antarctic, suggesting a global mode of interaction between atmosphere and ocean and consistent with GCM experiments of a proposed ENSO-NA

link [e.g., *Trenberth et al.*, 1998; *Dong et al.*, 2000; *Merkel and Latif*, 2002].

References

Allen, M. R., and L. A. Smith (1996), Monte Carlo SSA, detecting irregular oscillations in the presence of coloured noise, *J. Clim.*, *9*, 3383–3404.

Baldwin, M. P., and T. J. Dunkerton (2001), Stratospheric harbingers of anomalous weather regimes, *Science*, *294*, 581–584.

Capotondi, A., and M. A. Alexander (2001), Rossby waves in the tropical North Pacific and their role in decadal thermocline variability, *J. Phys. Oceanogr.*, *31*, 3496–3515.

Castanheira, J. M., and H.-F. Graf (2003), North Pacific–North Atlantic relationships under stratospheric control?, *J. Geophys. Res.*, *108*(D1), 4036, doi:10.1029/2002JD002754.

Clark, A. J. (1992), Low-frequency reflection from a nonmeriodional eastern ocean boundary and the use of coastal sea level to monitor eastern Pacific equatorial Kelvin waves, *J. Phys. Oceanogr.*, *22*, 163–183.

Dickey, J. O., S. L. Marcus, and O. Viron (2003), Coherent interannual and decadal variations in the atmosphere-ocean system, *Geophys. Res. Lett.*, *30*(11), 1573, doi:10.1029/2002GL016763.

Dong, B.-W., R. T. Sutton, S. P. Jewson, A. O'Neil, and J. M. Slingo (2000), Predictable winter climate in the North Atlantic sector during the 1997–1999 ENSO cycle, *Geophys. Res. Lett.*, *27*, 985–988.

Enfield, D. B., and J. S. Allen (1980), On the structure and dynamics of monthly mean sea level anomalies along the Pacific coast of North and South America, *J. Phys. Oceanogr.*, *10*, 557–578.

Fischer, H., F. Traufetter, H. Oerter, R. Weller, and H. Miller (2004), Prevalence of the Antarctic Circumpolar Wave over the last two millennia recorded in Dronning Maud Land ice, *Geophys. Res. Let.*, *31*, L08202, doi:10.1029/2003GL019186.

Foufoula-Georgiou, E., and K. Kumar (1995), *Wavelets in Geophysics*, 373 pp., Elsevier, New York.

Gloersen, R. (1995), Modulation of hemispheric sea-ice cover by ENSO events, *Nature*, *373*, 503–505.

Huang, J., K. Higuchi, and A. Shabbar (1998), The relationship between the North Atlantic Oscillation and the ENSO, *Geophys. Res. Lett.*, *25*, 2707–2710.

Jevrejeva, S., and J. C. Moore (2001), Singular spectrum analysis of Baltic Sea ice conditions and large-scale atmospheric patterns since 1708, *Geophys. Res. Lett.*, *28*, 4503–4507.

Jevrejeva, S., J. C. Moore, and A. Grinsted (2003), Influence of the Arctic Oscillation and El Niño-Southern Oscillation (ENSO) on ice conditions in the Baltic Sea: The wavelet approach, *J. Geophys. Res.*, *108*(D21), 4677, doi:10.1029/2003JD003417.

Kaplan, A., M. A. Cane, Y. Kushnir, A. C. Clement, M. B. Blumenthal, and B. Rajagopalan (1998), Analyses of global sea surface temperature 1856–1991, *J. Geophys. Res.*, *103*, 18,567–18,589.

Merkel, U., and M. Latif (2002), A high resolution AGCM study of the El Niño impact on the North Atlantic/European sector, *Geophys. Res. Lett.*, *29*(9), 1291, doi:10.1029/2001GL013726.

Meyers, S. D., A. Melsom, G. T. Mitchum, and J. J. O'Brien (1998), Detection of the fast Kelvin waves teleconnection due to El Niño Southern Oscillation, *J. Geophys. Res.*, *103*, 27,655–27,663.

Park, Y.-H., F. Roquet, and F. Vivier (2004), Quasi-stationary ENSO wave signals versus the Antarctic Circumpolar Wave scenario, *Geophys. Res. Lett.*, *31*, L09315, doi:10.1029/2004GL019806.

Pozo-Vázquez, D., M. J. Esteban-Parra, F. S. Rodrigo, and Y. Castro-Diez (2001), The association between ENSO and winter atmospheric circulation and temperature in the North Atlantic region, *J. Clim.*, *14*, 3408–3420.

Ribera, P., and M. Mann (2002), Interannual variability in the NCEP reanalysis 1948–1999, *Geophys. Res. Lett.*, *29*(10), 1494, doi:10.1029/2001GL013905.

Ropelewski, C. F., and P. D. Jones (1987), An extension of the Tahiti-Darwin Southern Oscillation Index, *Mon. Weather Rev.*, *115*, 2161–2165.

Seinä, A., and E. Palosuo (1996), The classification of the maximum annual extent of ice cover in the Baltic Sea 1720–1995, *Rep. Ser. 27*, pp. 79–91, Finn. Inst. Mar. Res., Helsinki.

Smith, T. M., and R. W. Reynolds (2003), Extended reconstruction of global sea surface temperatures based on COADS data (1854–1997), *J. Clim.*, *16*, 1495–1510.

Suginohara, N. (1981), Propagation of coastal-trapped waves at low latitudes in a stratified ocean with continental shelf slope, *J. Phys. Oceanogr.*, *11*, 1113–1122.

Thompson, D. W. J., and J. M. Wallace (1998), The Arctic Oscillation signature in the winter geopotential height and temperature fields, *Geophys. Res. Lett.*, *25*, 1297–1300.

Torrence, C., and P. Webster (1999), Interdecadal changes in the ENSO-monsoon system, *J. Clim.*, *12*, 2679–2690.

Trenberth, K. E., W. Branstator, D. Karoly, A. Kumar, N. Lau, and C. Ropelewski (1998), Progress during TOGA in understanding and modeling global teleconnections associated with tropical sea surface temperatures, *J. Geophys. Res.*, *103*, 14,291–14,324.

Venegas, S. A., and L. A. Mysak (2000), Is there a dominant timescale of natural climate variability in the Arctic?, *J. Clim.*, *13*, 3412–3434.

Venje, T. (2001), Anomalies and trends of sea ice extent and atmospheric circulation in the Nordic Seas during the period 1864–1998, *J. Clim.*, *14*, 255–267.

Wang, C., and R. H. Weisberg (1994), On the "slow mode" mechanism in ENSO- related coupled ocean-atmosphere models, *J. Clim.*, *7*, 1657–1667.

White, W. B., and Y. M. Tourre (2003), Global SST/SLP waves during the 20th century, *Geophys. Res. Lett.*, *30*(12), 1651, doi:10.1029/2003GL017055.

White, W. B., Y. M. Tourre, M. Barlow, and M. Dettinger (2003), A delayed action oscillator shared by biennial, interannual, and decadal signals in the Pacific Basin, *J. Geophys. Res.*, *108*(C3), 3070, doi:10.1029/2002JC001490.

———————————

A. Grinsted and J. C. Moore, Arctic Centre, University of Lapland, FIN-96101 Rovaniemi, Finland.

S. Jevrejeva, Proudman Oceanographic Laboratory, Birkenhead CH43 7RA, UK. (sveta@pol.ac.uk)